Journal of Diabetes

Journal of Diabetes **7** (2015) 360–368

ORIGINAL ARTICLE

Emodin up-regulates glucose metabolism, decreases lipolysis, and attenuates inflammation in vitro

Xiaoyan ZHANG,[1]* Rong ZHANG,[1,2]* Pengfei LV,[1] Jian YANG,[1] Yujie DENG,[1] Jun XU,[1] Rongfeng ZHU,[1] Di ZHANG[1] and Ying YANG[1]

[1]Shanghai Institute of Endocrine and Metabolic Diseases, Shanghai Clinical Center for Endocrine and Metabolic Diseases, Ruijin Hospital, Shanghai Jiaotong University School of Medicine, Shanghai, and [2]Peace Hospital Affiliated to Changzhi Medical College, Changzhi, China

Correspondence
Ying Yang, Shanghai Institute of Endocrine and Metabolic Diseases, Shanghai Clinical Center for Endocrine and Metabolic Diseases, Ruijin Hospital, Shanghai Jiaotong University School of Medicine, 197 Ruijin Road, Shanghai 200025, China.
Tel: +0086 021 6474 9885
Fax: +0086 021 6474 9885
Email: yangying_sh@yahoo.com

*Xiaoyan ZHANG and Rong ZHANG contribute equally to this work

Received 13 March 2014; revised 15 June 2014; accepted 22 June 2014.

doi: 10.1111/1753-0407.12190

Abstract

Background: Emodin, the major bioactive component of *Rheum palmatum*, has many different activities, including antitumor, anti-inflammatory, and antidiabetes effects. Recently, emodin was reported to regulate energy metabolism. In the present study, we further explored the effects of emodin on glucose and lipid metabolism.

Methods: Differentiated C2C12 myotubes and 3T3-L1 adipocytes were treated with or without different concentrations of emodin (6.25, 12.5, 25 or 50 μmol/L) for different time (1 h, 3 h, 12 h, 24 h or 48 h). Glucose metabolism, oxygen consumption, lactic acid levels, glycerol levels, and inflammation pathways were then evaluated. Cells were collected for quantitative polymerase chain reaction (PCR) and western blot analysis.

Results: Emodin upregulated glucose uptake and consumption in both C2C12 myotubes and 3T3-L1 adipocytes, with glycolysis increased. Furthermore, emodin inhibited lipolysis under basal conditions (as well as in the presence of 10 ng/ml tumor necrosis factor (TNF-)-α in 3T3-L1 adipocytes) and significantly decreased phosphorylated perilipin. Moreover, emodin inhibited the nuclear factor-κB and extracellular signal-regulated kinase pathways in C2C12 myotubes and 3T3-L1 adipocytes.

Conclusions: Emodin upregulates glucose metabolism, decreases lipolysis, and inhibits inflammation in C2C12 myotubes and 3T3-L1 adipocytes.

Keywords: emodin, glucose metabolism, inflammation, lipolysis.

Significant findings of the study: Emodin upregulates glucose metabolism by increasing AMP-activated protein kinase-mediated glycolysis, whereas perilipin participates in the negative regulation of lipolysis. Moreover, nuclear factor-κB and extracellular signal-regulated kinase were inhibited by emodin in both C2C12 myotubes and 3T3-L1 adipocytes.
What this study adds: The findings of the present study of the effects of emodin on glucose and lipid metabolism may provide further insight into application of emodin in energy imbalance.

Introduction

Emodin, (1,3,8-trihydroxy-6-methylanthraquinone)c, a naturally occurring anthraquinone isolated from *Rheum palmatum*, has been used as a laxative since ancient times. With the increased attention to Chinese herbal medicine, studies have been performed on emodin. Many distinct characteristics of emodin have been reported, such as antitumor activity,[1,2] anti-inflammatory effects[3,4] and antidiabetes potential.[5] However, the underlying mechanism of action of emodin in glucose and lipid metabolism remains unclear.

In a previous study, emodin was found to be an activator of peroxisome proliferator-activated receptor (PPAR) γ, promoting adipocyte differentiation and glucose uptake in 3T3-L1 adipocytes.[6] These observa-

tions suggest that emodin may contribute to the maintenance of glucose metabolism in fat tissue. However, further research is needed to verify the role of emodin in energy metabolism. Studies so far have shown that emodin negatively regulates phosphatidylinositol 3-kinase (PI3K)/AKT in HeLa and HepG2 cells,[7,8] contributing to its antitumor effects. In addition, emodin has been reported to be a novel AMP-activated protein kinase (AMPK) activator.[9,10] Because PI3K/AKT and AMPK are considered important regulators of glucose metabolism, we hypothesized that PI3K/AKT or AMPK may mediate the regulation by emodin of glucose metabolism.

Some PPARγ activators, such as rosiglitazone, have been reported to regulate lipolysis and inhibit inflammation.[11,12] Because emodin has been identified as an activator of PPARγ, it would be of interest to determine whether emodin is involved in lipolysis and inflammation. Perilipin, a lipid droplet surface protein, plays a central role in lipid storage and fatty acid release. It has been reported that Breeding the Plin -/- alleles into Leprdb/db mice reverses the obesity,[13] highlighting the importance of perilipin in metabolic diseases. Although emodin has been reported to suppress stimulated lipolysis in adipose tissue,[14] whether perilipin is involved in this process remains unknown. Furthermore, inflammation has recently been reported as a novel mechanism for energy imbalance in the body.[15] Reducing inflammation may help improve energy metabolism disorders. Nuclear factor (NF)-κB and extracellular signal-regulated kinase (ERK), as inflammation-related pathways, have been inhibited by emodin in vitro and in vivo.[16,17]

In the present study, we focused on the effects of emodin on energy metabolism and found that emodin increased glucose consumption and reduced lipolysis in both C2C12 myotubes and 3T3-L1 adipocytes. Furthermore, AMPK-mediated glycolysis may contribute to the upregulation of glucose metabolism, whereas perilipin participates in the negative regulation of lipolysis. Furthermore, we found that both NF-κB and ERK were inhibited by emodin in C2C12 myotubes and 3T3-L1 adipocytes.

Methods

Reagents and antibodies

RIPA lysis buffer, protease inhibitor, phosphatase inhibitor, emodin, dexamethasone (DEX), 3-isobutyl-1-methylxanthine (IBMX), triglyceride (TG) assay reagents and tumor necrosis factor-α (TNF) were obtained from Sigma (St Louis, MO, USA). Trizol was obtained from GIBCO-BRL (Grand Island, NY, USA), SuperScript III and oligo(dT) were from Invitrogen (Carlsbad, CA, USA), and 2-deoxy-D-[1-^{3}H]glucose (2-DG) was from Amersham (Buckinghamshire, UK). Recombinant human insulin was obtained from Lily (Fegersheim, France), whereas anti-total (t-) P65 and anti-phosphorylated (p-) P65 were obtained from Santa Cruz Biotechnology (Santa. Cruz, CA, USA). The other antibodies used in the present study (anti-GAPDH, anti-clathrin, anti-GLUT1, anti-GLUT4, anti-pACC(1-aminocyclopropane-1-carboxylic acid), anti-t-ACC, anti-p-AMPK, anti-t-AMPK, anti-t-ERK1/2, anti-p-ERK1/2, anti-p-(inhibitor of nuclear factor kappa-B kinase)IKKα/β, and anti-IκBα) were from Cell Signaling Technology (Beverly, MA, USA).

Cell culture

The C2C12 myotubes and 3T3-L1 adipocytes were purchased from America Cell Type Culture Collection (Manassas, VA, USA) and cultured in Dulbecco's modified Eagle's medium (DMEM) supplemented with 10% (v/v) fetal bovine serum (FBS) and 1%(v/v) antibiotic, in a humidified incubator with 5% CO_2 at 37°C. To obtain fully differentiated C2C12 myotubes, cells were grown to 60%–70% confluency and incubated for 4 days in the aforementioned medium containing only 2% (v/v) horse serum. To induce fully differentiated 3T3-L1 adipocytes, cells were incubated with Differentiation Medium A (DMEM supplemented with 10% FBS, 0.5 mmol/L IBMX, 1 μmol/L DEX, and 1.7 μmol/L insulin) for 48 h, when cell confluency reached 90%–100%, followed by incubation in Differentiation Medium B (DMEM supplemented with 10% FBS and 1.7 μmol/L insulin) for another 48 h.

Glucose uptake

After treatment, cells in 24-well plates were washed gently three times using Krebs'–Ringer phosphate buffer preheated to 37°C and incubated for 30 min in the above buffer. Then 50 μL Krebs'–Ringer phosphate buffer containing 1.85×104Bq/mL D-^{3}H-glucose was added to each well. After 10 min incubation, cells were washed three times rapidly with a solution of phosphate-buffered saline (PBS) containing 10 mmol/L glucose and then lysed using 0.1 mol/L NaOH containing 0.1% Triton X-100 for 45 min. Radioactivity were measured using a liquid scintillation counter.

Glucose consumption

Before experiments, mature C2C12 myotubes and 3T3-L1 adipocytes were cultured in DMEM containing 0.2% bovine serum albumin (BSA) and then treated with

or without 25 μmol/L emodin for 24 h. Glucose concentrations were determined using the glucose oxidase method. Glucose consumption was determined by subtracting the glucose concentration in cell wells from that of blank wells.

RNA extraction and real-time polymerase chain reaction

Total RNA was isolated from cells using Trizol reagent (GIBCO-BRL) according to the manufacturer's instructions and converted into cDNA using SuperScript III Reverse Transcriptase with 2 μg total RNA. Quantitative polymerase chain reaction (PCR) analysis was performed using SYBR Premix Ex Taq in a 7300 Quantitative PCR System (Applied Biosystems, Foster City, CA, USA). The primers used were as follows: GLUT1, 5′-CAT CCT TAT TGC CCA GGT GTT T-3′ (forward) and 5′-GAA GAC GAC ACT GAG CAG CAG A-3′ (reverse); GLUT4, 5′-CTT CTT TGA GAT TGG CCC TGG-3′ (forward) and 5′-AGG TGA AGA TGA AGA AGC CAA GC-3′ (reverse); and β-actin, 5′-CTG GGA CGA TAT GGA GAA GA-3′ (forward) and 5′-AGA GGC ATA CAG GGA CAA CA-3′ (reverse).

Western blot analysis

For western blot analysis, cells were harvested and suspended in ice-cold RIPA lysis buffer containing with 5 units/mL Proteinase Inhibitor Cocktail and 1 mmol/L phenylmethylsulphonyl fluoride for 30 min before being centrifuged at 12 000 g for 30 min at 4°C to obtain whole cell proteins. Proteins were separated by 12% sodium dodecyl sulfate–polyacrylamide gel electrophoresis and transferred to nitrocellulose membranes. The membranes were blocked with Tris-Hcl buffered saline (TBS) containing 1% Tween 20 (TBST) and 5% non-fat milk for 2 h, and then incubated with primary antibodies (diluted 1 : 1000) at 4°C overnight. After washing with TBST for three times, membranes were incubated with horseradish peroxidase-conjugated antibodies at room temperature for 1 h. Signals were detected using an enhanced chemiluminescence system (Pierce Biotechnology, Rockford, IL, USA).

Oxygen consumption

Differentiated cells were trypsinized and plated within a microtiter plate format embedded with an oxygen-sensitive dye in DMEM containing 10% FBS. After 6 h, 25 μmol/L emodin was added to the emodin-treated group. Oxygen consumption was determine in a BD Oxygen Biosensor System (BD Biosciences, San Jose, CA, USA). Fluorescence values were determined over a period of 1 h after 24 h treatment with emodin; the system expressed signals as normalized relative fluorescence units (NRFU).

Lactate assay

Cells in a 24-well plate were treated with or without 25 μmol/L emodin for 24 h in DMEM supplemented with 0.2% BSA before measurement. Lactate levels were determined using a commercially available lactate assay kit (Biomedical Research Service Center; Buffalo, NY, USA). Diluted culture media were mixed with the lactate assay solution and incubated at 37°C for 30 min. Absorbance was read at 492 nm for each sample and the lactate concentrations were deduced from a lactate standard curve.

Glycerol assay

Mature 3T3-L1 adipocytes were treated with different concentrations of emodin (6.25, 12.5, 25 or 50 μmol/L) or TNF-α (10 ng/ml) for 24 h before lipolysis assessment. Then, glycerol in the medium was measured using a glycerol 3-phosphate oxidase trinder kit (Sigma-Aldrich, St. Louis, MO, USA). Glycerol release was calculated by glycerol concentration divided by protein concentration.

Electrophoresis mobility shift assay

An electrophoretic mobility shift assay (EMSA) was performed as described previously[18]. Protein extracts (10 μg each) were incubated with radiolabelled probes for binding of active NF-κB for 30 min at room temperature. The probes used were oligonucleotides containing NF-κB binding sites (5′-AGTTGAGGGGACTTTCC CAGGC-3′, 3′-TCAACTCCCCTGAAAGGGTCCG-5′). The protein–DNA complexes were separated by electrophoresis on a native 5% acrylamide gel, and autoradiography was performed.

Statistical analysis

Data are present as the mean ± SD of three independent experiments. The significance of differences between groups was analyzed by two-tailed Student's t test. $P < 0.05$ was considered significant.

Results

Emodin upregulated glucose metabolism with increasing expression of GLUT1/4

Muscle and adipose tissue both play crucial roles in glucose metabolism, and evaluation of glucose

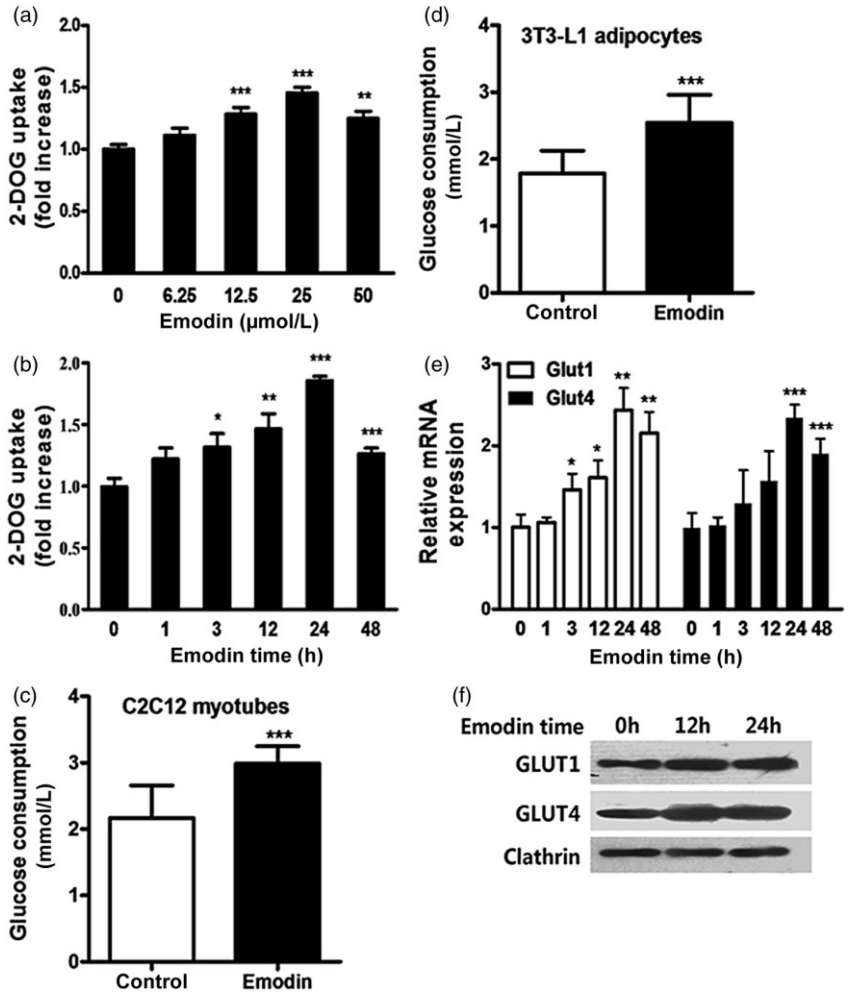

Figure 1 Emodin increased glucose uptake and expression of glucose transporters GLUT1 and GLUT4 in C2C12 myotubes, (a) Mature C2C12 myotubes were treated with different concentrations of emodin for 24 h, and glucose uptake was determined with 2-deoxy-D-[^{3}H]-glucose. (b) Time course of 2-deoxy-D-[^{3}H]-glucose uptake in mature C2C12 myotubes exposed to 25 μmol/L emodin for different times. (c,d) Mature C2C12 myotubes (c) and 3T3-L1 adipocytes (d) were treated with 25 μmol/L emodin for 24 h and glucose consumption was analyzed and compared with control. (e) Relative mRNA expression of GLUT1 and GLUT4 in C2C12 myotubes treated with 25 μmol/L emodin for the indicated time. (f) Protein levels of GLUT1 and GLUT4 in C2C12 myotubes treated with 25 μmol/L emodin for 0, 12, and 24 h. All values were the mean ± SD. $^*P < 0.05$, $^{**}P < 0.01$, $^{***}P < 0.001$ compared with control.

consumption and uptake is crucial in the study of glucose metabolism. Therefore, we focused on glucose uptake and consumption in C2C12 myotubes and 3T3-L1 adipocytes.

Mature C2C12 myotubes were treated with different concentrations of emodin (6.25, 12.5, 25 or 50 μmol/L) for 1 h, 3 h, 12 h, 24 h or 48 h, to enable evaluation of dose–response curves of the effect on emodin on glucose uptake (Fig. 1a) and the time course of the effects (Fig. 1b). Emodin significantly increased glucose uptake in C2C12 myotubes, with the concentration of 25 μmol/L and 24 h exposure having the greatest effect. In subsequent experiments, mature C2C12 myotubes (Fig. 1c) and 3T3-L1 adipocytes (Fig. 1d) were treated with 25 μmol/L emodin for 24 h and glucose consumption was analyzed in comparison with control. Glucose consumption increased significantly in emodin-treated cells, suggesting that emodin may upregulate glucose utilization. We further investigated expression of GLUT1/4, which are closely associated with glucose transportation and therefore may regulate glucose uptake. We found that mRNA levels of GLUT1/4 increased markedly in cells exposed to 25 μmol/L emodin for 24 h (Fig. 1e), which is in accordance with the observed changes in glucose uptake. Similarly, a significant increase in GLUT1/4 proteins was observed in C2C12 myotubes treated with 25 μmol/L emodin for 12 or 24 h (Fig. 1f). These results suggested that emodin increases glucose metabolism in C2C12 myotubes by upregulating the expression of GLUT1/4. Similar increases in glucose uptake and GLUT1/4 expression were seen in 3T3-L1 adipocytes, which has also been reported previously.[6]

Activation of the AMPK pathway by emodin in C2C12 myotubes and 3T3-L1 adipocytes

As reported[19] PI3K/AKT and AMPK are upstream of GLUT1/4, which is responsible for glucose transportation. To identify which pathway was involved in regula-

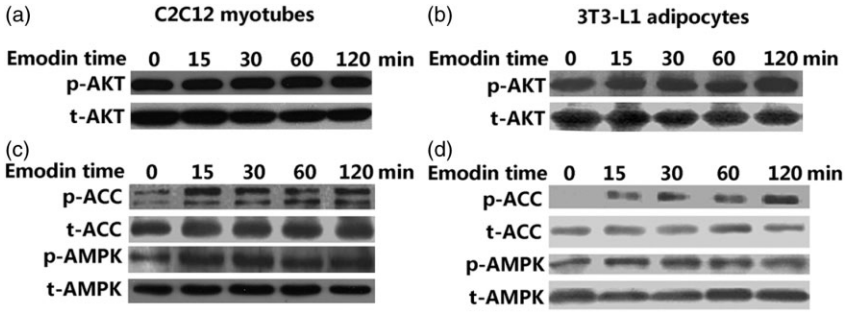

Figure 2 Effects of emodin on the AKT and AMP-activated protein kinase (AMPK)/ACC pathways in C2C12 myotubes and 3T3-L1 adipocytes. (a,c) Mature C2C12 myotubes were treated with 25 μmol/L emodin for different times and then AKT- (a) and AMPK/ACC-related proteins (c) were detected by western blot analysis. (b,d) Mature 3T3-L1 adipocytes were treated with 50 μmol/L emodin for different times and then western blot analysis was used to detect changes in AKT- (b) and AMPK/ACC-related proteins (d). p-, phosphorylated; t-, total.

tion of glucose homeostasis by emodin in C2C12 myotubes and 3T3-L1 adipocytes, PI3K/AKT- and AMPK-related proteins were detected by western blot analysis. No changes in p-AKT were observed in C2C12 myotubes (Fig. 2a) or 3T3-L1 adipocytes (Fig. 2b), suggesting that PI3K/AKT was less important in this process. However, the AMPK pathway was significantly activated after emodin treatment in C2C12 myotubes (Fig. 2c) and 3T3-L1 adipocytes (Fig. 2d), as evidenced by increases in p-ACC and p-AMPK. There were notable increases in both p-ACC and p-AMPK after only 15 min exposure to emodin. These data suggest that AMPK is mainly involved in the process of emodin regulation of glucose uptake.

Emodin decreased oxygen consumption in C2C12 myotubes and 3T3-L1 adipocytes

Because low oxygen is the most typical trigger of AMPK, we surmised that emodin may induce a low oxygen status and thus activate the AMPK pathway. Therefore, oxygen consumption was determined every 10 min in mature C2C12 myotubes (Fig. 3a) and 3T3-L1 adipocytes (Fig. 3b) exposed (or not) to 25 μmol/L emodin for 24 h. Compared with control, emodin inhibited oxygen consumption from 40 min in C2C12 myotubes and from 20 min in 3T3-L1 adipocytes. The slopes of the oxygen consumption vs time line graphs also indicated that emodin suppressed oxygen consumption in C2C12 myotubes and 3T3-L1 adipocytes. Together, these results demonstrate that emodin creates low oxygen conditions to activate AMPK.

Accumulation of lactic acid in emodin-treated C2C12 myotubes and 3T3-L1 adipocytes

The findings reported above suggest that emodin enhances glucose metabolism while inhibiting oxygen consumption. Thus, glycolysis, which always occurs under low oxygen conditions, may play an important

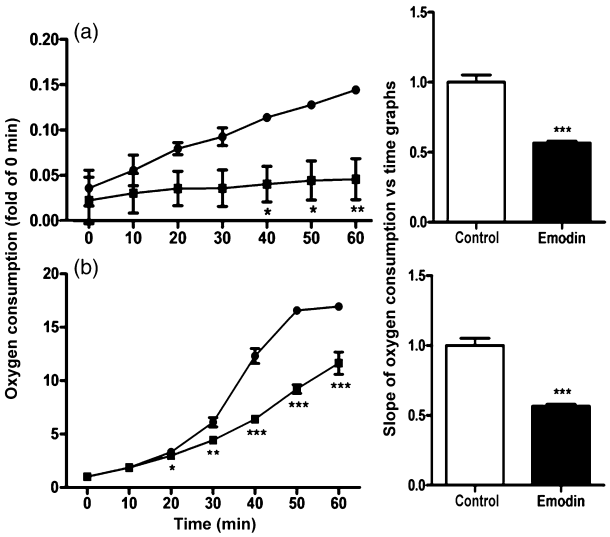

Figure 3 Emodin decreased oxygen consumption in C2C12 myotubes and 3T3-L1 adipocytes. (a) Mature C2C12 myotubes and (b) 3T3-L1 adipocytes were treated with or without 25 μmol/L emodin for 24 h and oxygen consumption was recorded every 10 min. Data in the control group (&U25CF;) and emodin-treated (■) groups are shown as both line graphs (oxygen consumption vs time) and histograms. Data are the mean ± SD. $*P < 0.05$, $**P < 0.01$, $***P < 0.001$ (paired *t*-test).

role in the process. Lactic acid levels were determined as an indicator of changes in glycolysis. Compared with control, lactic acid levels in C2C12 myotubes (Fig. 4a) and 3T3-L1 adipocytes (Fig. 4b) both increased. These results suggest that glycolysis may mediate the upregulation in glucose metabolism.

Emodin inhibited lipolysis in 3T3-L1 adipocytes

Next, we evaluated the effect of emodin on lipolysis. Glycerol levels, direct indicators of the lipolytic process, were determined and the effects of emodin on basal and induced lipolysis were investigated. First, 3T3-L1 adipo-

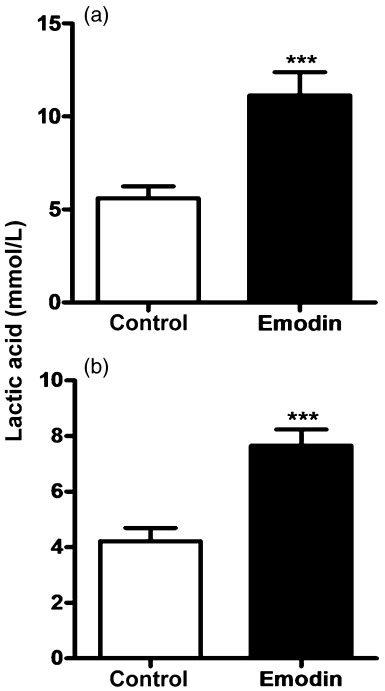

Figure 4 Emodin increased lactic acid levels in C2C12 myotubes and 3T3-L1 adipocytes. (a) Mature C2C12 myotubes and (b) 3T3-L1 adipocytes were treated with 225 μmol/L emodin for 24 h and lactic acid levels were analyzed. Data are the mean ± SD. $***P < 0.001$ compared with control.

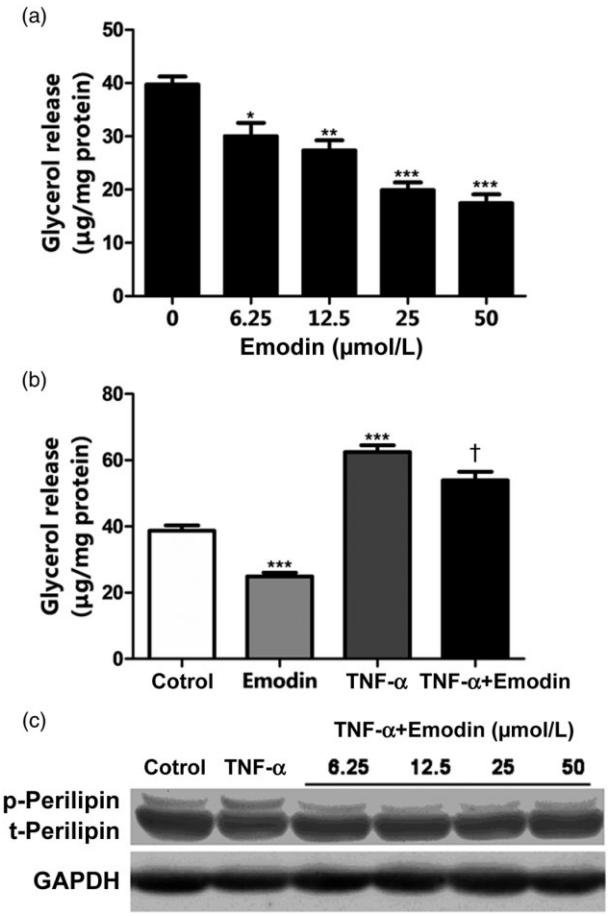

Figure 5 Emodin inhibited lipolysis in 3T3-L1 adipocytes. (a) Glycerol levels were detected in 3T3-L1 adipocytes treated with different concentrations of emodin for 24 h. (b) 3T3-L1 adipocytes were treated with or without emodin (50 μmol/L, 24 h) and tumor necrosis factor (TNF)-α (10 ng/mL, 30 min), and glycerol levels were determined. (c) 3T3-L1 adipocytes were treated with different concentrations of emodin for 24 h. Western blot analysis was then performed using anti-perilipin and anti-GAPDH antibodies. p-, phosphorylated; t-, total. Data are the mean ± SD. $*P < 0.05$, $**P < 0.01$, $***P < 0.001$ compared with control; $^{\dagger}P < 0.05$ compared with TNF-α alone.

cytes were exposed to different concentrations of emodin (6.25, 12.5, 25 or 50 μmol/L) for 24 h to construct a dose–response curve (Fig. 5a). Emodin inhibited lipolysis at a minimum concentration of 6.25 μmol/L, with 50 μmol/L emodin exerting the most potent inhibitory action. Then, 10 ng/ml TNF-α was used to induce lipolysis, with emodin added (or not) 3 h in advance (Fig. 5b). The TNF-α-induced lipolysis was significantly suppressed by emodin, suggesting that both basal and induced lipolysis were inhibited by emodin in 3T3-L1 adipocytes.

There were significant changes in p-perilipin, which is closely related to lipolysis, in cells treated with 10 ng/ml TNF-α and emodin at 6.25, 12.5, 25 or 50 μmol/L (Fig. 5c). The significant increase in p-perilipin induced by TNF-α was markedly reduced by emodin. These observations are consistent with the aforementioned findings and suggest that perilipin may play an important role in the effect of emodin in suppressing lipolysis.

Emodin rescued TNF-α-induced inflammation in C2C12 myotubes and 3T3-L1 adipocytes

The anti-inflammatory effects of emodin were also investigated in C2C12 myotubes and 3T3-L1 adipocytes exposed to 10 ng/ml TNF-α for 30 min to activate the NF-κB and ERK pathways. After 25 μmol/L emodin treatment, NF-κB- and ERK-related proteins were measured by western blot analysis. Expression of P65 and IKKα/β was markedly decreased in C2C12 myotubes (Fig. 6a) and 3T3-L1 adipocytes (Fig. 6b) treated with emodin, whereas IκBα (an NF-κB inhibitor) was activated. Similarly, emodin inhibited the ERK pathway in both C2C12 myotubes (Fig. 6c) and 3T3-L1 adipocytes (Fig. 6d). Emodin treatment significantly attenuated activation of NF-κB (Fig. 6e).

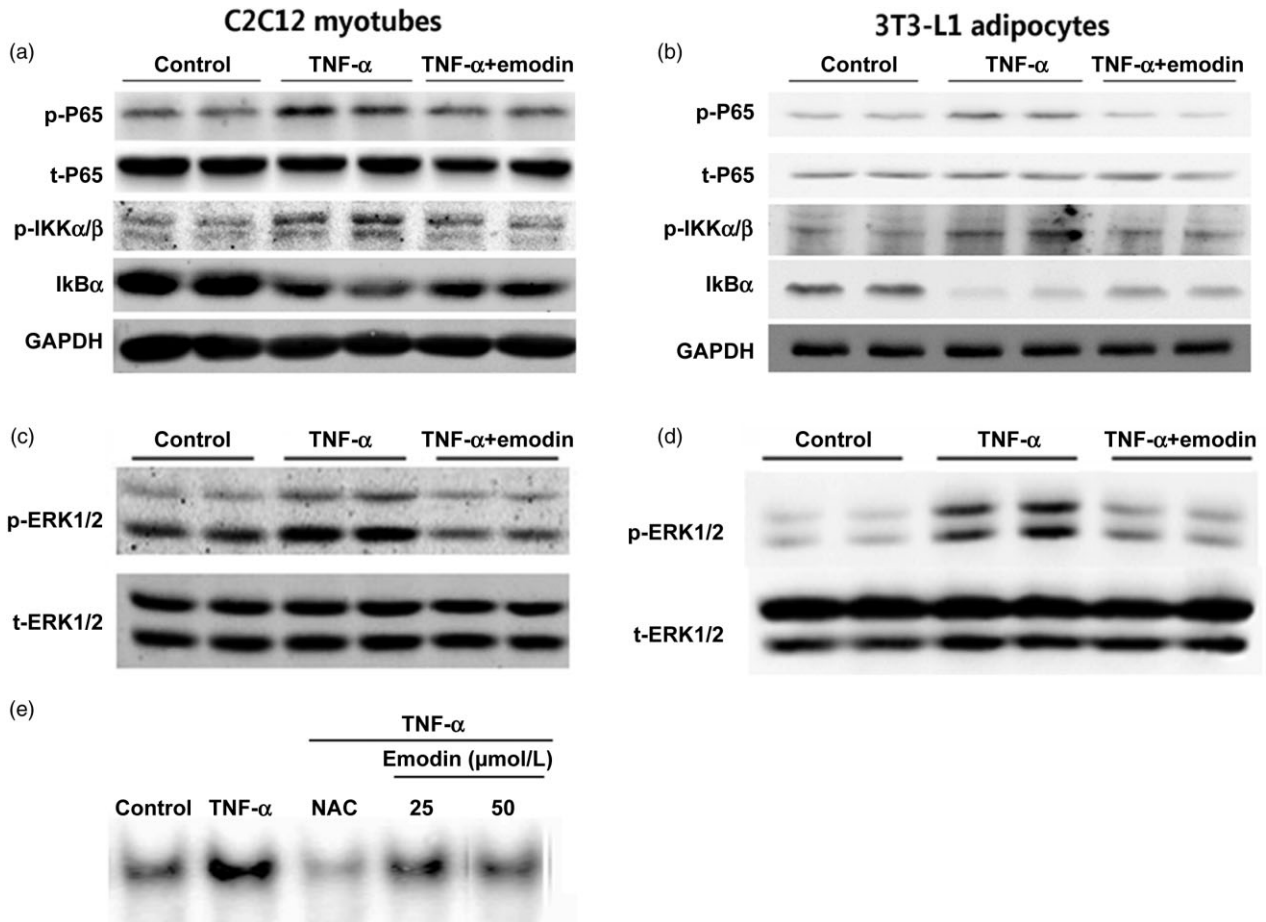

Figure 6 Emodin improved inflammation in C2C12 myotubes and 3T3-L1 adipocytes. (a) Mature C2C12 myotubes and (b) 3T3-L1 adipocytes were treated with or without emodin (25 μmol/L, 3 h) and tumor necrosis factor (TNF)-α (10 ng/mL, 30 min) and subjected to western blot analysis using anti-phosphorylated (p-) P65, anti-total (t-) P65, anti-p-IKKα/β (inhibitor of nuclear factor kappa-B kinase subunit α/β), anti-IκBα and anti-GAPDH antibodies. (c) Mature C2C12 cells and (d) 3T3-L1 adipocytes were treated as described above and subjected to western blot analysis using anti-p-extracellular signal-regulated kinase (ERK) 1/2 and anti-t-ERK1/2 antibodies. (e) Mature 3T3-L1 adipocytes were treated with or without different concentrations of emodin (3 h) and TNF-α (10 ng/mL, 30 min), then subjected to an electrophoretic mobility shift assay performed using nuclear factor-κB as a probe. NAC, positive control.

Discussion

Data from the present study support the notion that emodin has a positive effect on glucose metabolism in C2C12 myotubes and 3T3-L1 adipocytes, which is due primarily to increases in glycolysis and may be mediated by the AMPK signaling pathway. Furthermore, we found that emodin reduced lipolysis and that perilipin was involved in this process. Moreover, an anti-inflammatory effect of emodin on NF-κB and ERK was demonstrated.

Aerobic respiration and glycolysis together regulate glucose utilization. Decreased oxygen consumption always promotes an energy switch from aerobic respiration to glycolysis. Anaerobic glycolysis is stimulated by many factors, including insulin-like growth factor-1,[20] berberine,[21] epinephrine,[22] and excitatory amino acids,[23] with more lactic acid produced. In the present study, we found that glucose consumption was increased in emodin-treated C2C12 myotubes and 3T3-L1 adipocytes, and that glucose uptake and the expression of GLUT1/4 were induced by emodin in C2C12 myotubes, with obvious accumulation of lactic acid. Thus, emodin may increase glucose metabolism in C2C12 myotubes and 3T3-L1 adipocytes via glycolysis.

It has been reported that AMPK, a highly conserved sensor of energy status, increases GLUT1/4 levels and mediates glucose uptake.[24–26] Because emodin activated AMPK, the relationship between emodin and energy status is of interest. Recently, Song et al.[27] reported that emodin regulates glucose utilization by activating AMPK in skeletal muscle and liver cells. In the present study, an

AMPK signaling pathway was detected in emodin-treated C2C12 myotubes and 3T3-L1 adipocytes, indicating that AMPK-mediated glycolysis may be a potential mechanism for the regulation of glucose metabolism in muscle and adipose tissues. These results are consistent with those of Song et al.[27] and further revealed the links among emodin, AMPK, and glycolysis.

Lipolysis, another key point of energy metabolism, was also investigated in the present study. First, we confirmed that emodin inhibited lipolysis under basal conditions and in the presence of TNF-α. Then, we found that decreases in perilipin, a protein closely related to lipid metabolism and obesity,[13,28,29] may be a potential mechanism leading to inhibition of lipolysis in 3T3-L1 adipocytes exposed to emodin.

It has been reported that the anti-inflammatory effect of rosiglitazone is not mediated by PPARγ or AMPK.[30] However, it has also been reported that rosiglitazone resolves inflammation mediated by PPARγ[31] or phosphatase and tensin homolog (PTEN)-dependent pathways.[32] Emodin, as a PPARγ agonist, should have similar effects to rosiglitazone. Herein, we found that TNF-α-induced activation of NF-κB and ERK was inhibited by emodin in C2C12 myotubes and 3T3-L1 adipocytes. Further studies are needed to determine whether AMPK and/or PPARγ pathways are associated with the capacity of emodin to repress inflammatory responses induced by the NF-κB system.

Together, our findings indicate that emodin activates AMPK, downregulates perilipin, and inhibits NF-κB and ERK, thereby increasing glycolysis and glucose metabolism and suppressing lipolysis and inflammation. These data may help our understanding of the role emodin in energy metabolism, and provide a new understanding in the application of herbal medicine. However, more in vivo and clinical research is required to further investigate the precise mechanisms underlying these effects.

Acknowledgment

This work was supported by grants from National Natural Scientific Foundation of China (81100604 and 81170799).

Disclosure

The authors have no conflicts of interest to declare.

References

1. Cha TL, Qiu L, Chen CT, Wen Y, Hung MC. Emodin down-regulates androgen receptor and inhibits prostate cancer cell growth. *Cancer Res*. 2005; **65**: 2287–95.
2. Huang Q, Lu G, Shen HM, Chung M, Ong CN. Anti-cancer properties of anthraquinones from rhubarb. *Med Res Rev*. 2007; **27**: 609–30.
3. Kuo YC, Meng HC, Tsai WJ. Regulation of cell proliferation, inflammatory cytokine production and calcium mobilization in primary human T lymphocytes by emodin from *Polygonum hypoleucum* Ohwi. *Inflamm Res*. 2001; **50**: 73–82.
4. Kumar A, Dhawan S, Aggarwal BB. Emodin (3-methyl-1,6,8-trihydroxyanthraquinone) inhibits TNF-α-induced NF-kappaB activation, IkappaB degradation, and expression of cell surface adhesion proteins in human vascular endothelial cells. *Oncogene*. 1998; **17**: 913–8.
5. Xue J, Ding W, Liu Y. Anti-diabetic effects of emodin involved in the activation of PPARγ on high-fat diet-fed and low dose of streptozotocin-induced diabetic mice. *Fitoterapia*. 2010; **81**: 173–7.
6. Yang Y, Shang W, Zhou L, Jiang B, Jin H, Chen M. Emodin with PPARγ ligand-binding activity promotes adipocyte differentiation and increases glucose uptake in 3T3-Ll cells. *Biochem Biophys Res Commun*. 2007; **353**: 225–30.
7. Olsen BB, Bjørling-Poulsen M, Guerra B. Emodin negatively affects the phosphoinositide 3-kinase/AKT signalling pathway: A study on its mechanism of action. *Int J Biochem Cell Biol*. 2007; **39**: 227–37.
8. Huang Q, Shen HM, Ong CN. Emodin inhibits tumor cell migration through suppression of the phosphatidylinositol 3-kinase-Cdc42/Rac1 pathway. *Cell Mol Life Sci*. 2005; **62**: 1167–75.
9. Chen Z, Zhang L, Yi J, Yang Z, Zhang Z, Li Z. Promotion of adiponectin multimerization by emodin: A novel AMPK activator with PPARγ agonist activity. *J Cell Biochem*. 2012; **113**: 3547–58.
10. Tzeng TF, Lu HJ, Liou SS, Chang CJ, Liu IM. Emodin, a naturally occurring anthraquinone derivative, ameliorates dyslipidemia by activating AMP-activated protein kinase in high-fat-diet-fed rats. *Evid Based Complement Alternat Med*. 2012; **2012**: 781812.
11. Wang P, Renes J, Bouwman F, Bunschoten A, Mariman E, Keijer J. Absence of an adipogenic effect of rosiglitazone on mature 3T3-L1 adipocytes: Increase of lipid catabolism and reduction of adipokine expression. *Diabetologia*. 2007; **50**: 654–65.
12. Abdin AA, Baalash AA, Hamooda HE. Effects of rosiglitazone and aspirin on experimental model of induced type 2 diabetes in rats: Focus on insulin resistance and inflammatory markers. *J Diabetes Complications*. 2010; **24**: 168–78.
13. Martinez-Botas J, Anderson JB, Tessier D et al. Absence of perilipin results in leanness and reverses obesity in Leprdb/dbmice. *Nat Genet*. 2000; **26**: 474–9.
14. Wang YJ, Huang SL, Feng Y, Ning MM, Leng Y. Emodin, an 11β-hydroxysteroid dehydrogenase type 1 inhibitor, regulates adipocyte function in vitro and exerts anti-diabetic effect in ob/ob mice. *Acta Pharmacol Sin*. 2012; **33**: 1195–203.
15. Ye J, Keller JN. Regulation of energy metabolism by inflammation: A feedback response in obesity and calorie restriction. *Aging (Albany)*. 2010; **2**: 361–8.

16. Li D, Zhang N, Cao Y et al. Emodin ameliorates lipopolysaccharide-induced mastitis in mice by inhibiting activation of NF-κB and MAPKs signal pathways. *Eur J Pharmacol*. 2013; **705**: 79–85.
17. Li HL, Chen HL, Li H et al. Regulatory effects of emodin on NF-κB activation and inflammatory cytokine expression in RAW 264.7 macrophages. *Int J Mol Med*. 2005; **16**: 41–7.
18. Juvekar A, Ramaswami S, Manna S, Chang TP, Zubair A, Vancurova I. Electrophoretic mobility shift assay analysis of NFκB transcriptional regulation by nuclear IκBα. *Methods Mol Biol*. 2012; **809**: 49–62.
19. Huang YC, Chang WL, Huang SF, Lin HC, Chang TC. Pachymic acid stimulates glucose uptake through enhanced GLUT4 expression and translocation. *Eur J Pharmacol*. 2010; **648**: 39–49.
20. Semsarian C, Sutrave P, Richmond DR, Graham RM. Insulin-like growth factor (IGF-I) induces myotube hypertrophy associated with an increase in anaerobic glycolysis in a clonal skeletal-muscle cell model. *Biochem J*. 1999; **339**: 443–51.
21. Yin J, Gao Z, Liu D, Liu Z, Ye J. Berberine improves glucose metabolism through induction of glycolysis. Am. J. Physiol. *Endocrinol Metab*. 2008; **294**: E148–56.
22. James JH, Wagner KR, King JK et al. Stimulation of both aerobic glycolysis and Na^+-K^+-ATPase activity in skeletal muscle by epinephrine or amylin. *Am J Physiol*. 1999; **277**: E176–86.
23. Pellerin L, Magistretti P. Excitatory amino acids stimulate aerobic glycolysis in astrocytes via an activation of the Na^+/K^+ ATPase. *Dev Neurosci*. 1996; **18**: 336–42.
24. Russell RR, Bergeron R, Shulman GI, Young LH. Translocation of myocardial GLUT-4 and increased glucose uptake through activation of AMPK by AICAR. *Am J Physiol*. 1999; **277**: H643–9.
25. Sambandam N, Lopaschuk GD. AMP-activated protein kinase (AMPK) control of fatty acid and glucose metabolism in the ischemic heart. *Prog Lipid Res*. 2003; **42**: 38–256.
26. Abbud W, Habinowski S, Zhang JZ et al. Stimulation of AMP-activated protein kinase (AMPK) is associated with enhancement of Glut1-mediated glucose transport. *Arch Biochem Biophys*. 2000; **380**: 347–52.
27. Song P, Kim JH, Ghim J et al. Emodin regulates glucose utilization by activating AMP-activated protein kinase. Journal of. *Biol Chem*. 2013; **288**: 5732–42.
28. Tansey J, Sztalryd C, Gruia-Gray J et al. Perilipin ablation results in a lean mouse with aberrant adipocyte lipolysis, enhanced leptin production, and resistance to diet-induced obesity. *Proc Natl Acad Sci USA*. 2001; **98**: 6494–9.
29. Greenberg AS, Egan JJ, Wek SA, Garty NB, Blanchette-Mackie E, Londos C. Perilipin, a major hormonally regulated adipocyte-specific phosphoprotein associated with the periphery of lipid storage droplets. Journal of. *Biol Chem*. 1991; **266**: 11341–6.
30. Zhu M, Flynt L, Ghosh S et al. Anti-inflammatory effects of thiazolidinediones in human airway smooth muscle cells. *Am J Respir Cell Mol Biol*. 2011; **45**: 111–19.
31. Ballesteros I, Cuartero MI, Pradillo JM et al. Rosiglitazone-induced CD36 upregulation resolves inflammation by PPARgamma and 5-LO-dependent pathways. *J Leukoc Biol*. 2014; **95**: 587–98.
32. Lin CF, Young KC, Bai CH et al. Rosiglitazone regulates anti-inflammation and growth inhibition via PTEN. *Biomed Res Int*. 2014; **2014**: 787924.